

Toward Robust Semi-supervised Regression via Dual-stream Knowledge Distillation

Ye Su¹, Hezhe Qiao^{2*}, Wei Huang³ and Lin Chen^{1*}

¹Chongqing Institute of Green and Intelligent Technology, Chinese Academy of Sciences

²Singapore Management University

³Beijing University of Posts and Telecommunications

suye@cigit.ac.cn, hezheqiao.2022@phdcs.smu.edu.sg, huangwei@bupt.edu.cn, chenlin@cigit.ac.cn

Abstract

Semi-supervised regression (SSR), which aims to predict continuous scores of samples while reducing reliance on a large amount of labeled data, has recently received considerable attention across various applications, including computer vision, natural language processing, and audio and medical analysis. Existing SSR methods typically train models on scarce labeled data by introducing constraint-based regularization or ordinal ranking to reduce overfitting. However, these approaches fail to fully exploit the abundance of unlabeled samples. While consistency-driven pseudo-labeling methods attempt to incorporate unlabeled data, they are highly sensitive to pseudo-label quality and noisy predictions. To address these challenges, we introduce a **Dual-stream Knowledge Distillation framework (DKD)**, which is specially designed for the SSR task to distill knowledge from both continuous-valued knowledge and distribution information, better preserving regression magnitude information and improving sample efficiency. Specifically, in DKD, the teacher is optimized solely with ground-truth labels for label distribution estimation, while the student learns from a mixture of real labels and teacher-generated pseudo targets on unlabeled data. The distillation design ensures the effective supervision transfer, allowing the student to leverage pseudo labels more robustly. Then, we introduce an advanced Decoupled Distribution Alignment (DDA) to align the target class and non-target class between teacher and student on the distribution, enhancing the student’s capacity to mitigate noise in pseudo-label supervision and learn a more well-calibrated regression predictor. Extensive experiments were conducted on diverse datasets, including audio, text, image, and medical data. We show that DKD exhibits strong generalization capabilities and outperforms the best competing methods by 4.97% and 11.81% in terms of overall MAE and R^2 , respectively.

*Corresponding authors.

1 Introduction

Semi-supervised regression (SSR) aims to rank or predict continuous scores of samples while reducing reliance on a large amount of labeled data. It has been widely applied in various scenarios, including age estimation, clinical score prediction, and audio-based assessments, and other real-world applications where a large amount of labeled data across diverse are difficult to obtain [Ren *et al.*, 2022; Gui *et al.*, 2024; Bao *et al.*, 2024]. With the rapid advancement of deep learning in recent years, regression tasks using deep learning models across various domains have attracted significant attention [Yang *et al.*, 2024; Van Engelen and Hoos, 2020], especially in the SSR task. Some approaches directly employ deep learning models such as CNNs for images and RNNs for time series, optimizing them with loss functions like Mean Squared Error (MSE) or Mean Absolute Error (MAE) on the available labeled data [Mohammadi Foumani *et al.*, 2024; Yang *et al.*, 2022; Zhang *et al.*, 2017a]. However, such a straightforward application struggles to learn effective patterns in scenarios with scarce labeled data, owing to the heavy reliance of deep learning models on large-scale annotations [Pan *et al.*, 2024; Yin *et al.*, 2022]. Therefore, direct regression (DR) based models typically yield suboptimal performance.

To exploit the abundance of unlabeled data, several consistency-driven pseudo-labeling methods that assign the pseudo-labels on the unlabeled samples have been proposed [Zhang *et al.*, 2025; Zheng *et al.*, 2025]. Pseudo-labels are typically generated by training on the available labeled samples, and consistency regularization is often used to assist the optimization process and pseudo-labeling [Zhao *et al.*, 2025; Zhao and Wen, 2025]. While pseudo-labeling helps mitigate the challenge of limited labeled data, as some predicted incorrect labels are directly treated as true labels during training, and the model is likely to overfit to the wrong annotations. Therefore, the effectiveness of these approaches heavily relies on the quality of the pseudo-labels [Jo *et al.*, 2024; Yin *et al.*, 2022], and assessing the reliability of the generated pseudo-labels remains a challenging task.

To address these challenges, we introduce an advanced decoupled distillation framework (DKD), specifically designed for SSR, to effectively exploit unlabeled samples. DKD distills the knowledge from both continuous-valued knowledge and distribution information in an end-to-end manner, bet-

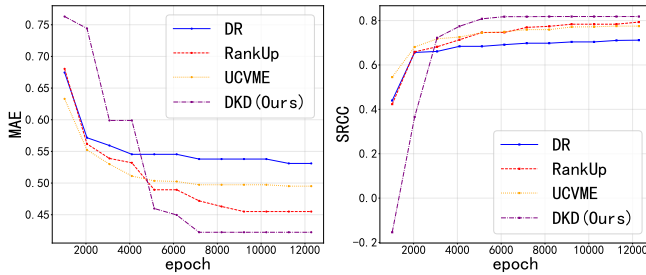


Figure 1: MAE and test SRCC curves for direct regression (DR), Rankup, UCVME, and DKD on the BVCC dataset. Rankup yields the least competitive results, as its pairwise ranking method may not fully capture the continuous relationships. Although UCVME improves performance via consistency-constrained pseudo-labels, it still falls short of DKD.

ter preserving regression magnitude information and improving sample efficiency. Specifically, DKD is implemented by a teacher model optimized solely with ground-truth labels for label distribution learning, producing informative predictions, while the student learns from a mixture of real labels and teacher-generated pseudo scores on unlabeled data, ensuring effective supervision transfer. The distillation allows the student to leverage pseudo labels more robustly, mitigating the interference from noisy pseudo-supervision in SSR. We further introduce an advanced decoupling distribution alignment (DDA) approach to distill the distribution information from the labeled trained teacher model, where we decouple the distribution into two parts for alignment, rather than aligning the distribution directly. DDA aligns the target and non-target distributions between the teacher and student in a decoupled manner, with an adaptive learnable weighting scheme, thereby enabling the student to better exploit unlabeled samples while reducing overfitting to noisy pseudo-labels and learning a more well-calibrated regression model. As shown in the Fig 1, the DKD can learn more robust and more generalizable knowledge representation provided by the mixture of labeled and pseudo-labeled samples provided by the teacher model. It outperforms the conventional method, direct regression (DR), and strong competing methods, including RankUp [Huang *et al.*, 2024], UCVME [Dai *et al.*, 2023a], achieving the best performance on both MAE and SRCC. In summary, this work makes the following main contributions.

- We propose DKD, the first end-to-end decoupled distillation framework for semi-supervised regression, which effectively directly distills both continuous-valued knowledge and distribution information in an end-to-end manner, better preserving regression magnitude information and improving sample efficiency under limited labels.
- We further introduce a novel alignment method, block-aware decouple distribution alignment (DDA), which enables the student model to identify important classes, enhancing the student’s capacity to mitigate noise in pseudo-label supervision and learn a more well-calibrated regression predictor.

- Extensive experiments were conducted on the datasets from various domains, including audio, text, image, and medical data. The experimental results demonstrate that DKD outperforms the state-of-the-art semi-supervised regression methods.

2 Related Works

2.1 Semi-supervised Regression

The SSR methods can be roughly categorized into pseudo-label-based methods, consistency regularization, and contrastive-learning-based methods. Jo *et al.* [Jo *et al.*, 2024] propose an SSR framework that uses uncertainty estimation to guide pseudo-labeling, alongside a pseudo-label calibration approach that enhances pseudo-label quality by propagating information from labeled to unlabeled samples. Semi-supervised deep kernel learning [Jean *et al.*, 2018] minimizes predictive variance on unlabeled data through consistency regularization, leveraging the robust uncertainty quantification provided by Gaussian processes. Some contrastive-learning-based methods exploit the ranking information among samples as auxiliary for regression [Qiao *et al.*, 2022; Huang *et al.*, 2024]. For example, RankUp [Huang *et al.*, 2024] constructs pairwise ranking labels from continuous targets with an auxiliary ranking classifier. CLSS [Dai *et al.*, 2023a] and GCLSS [Wang *et al.*, 2025] facilitate contrastive regression by exploiting the ordinal relationships between unlabeled samples with a spectral seriation algorithm.

Although these methods have achieved remarkable success in SSR, most of them do not fully leverage the potential of abundant unlabeled data. Pseudo-labeling approaches incorporate unlabeled samples into training, but they are often sensitive to noisy pseudo-targets and may even degrade performance. In DKD, we propose an advanced decoupled representation distillation strategy that transfers knowledge from both continuous-value supervision and distributional information, enabling effective utilization of both pseudo-labeled and ground-truth labeled samples.

2.2 Distribution Alignment in Distillation

Distribution alignment is a strategy used during student model training to match not only the outputs of the teacher model but also its underlying distributions. Existing approaches can be roughly categorized into logit-level alignment and feature-level alignment. Logit-level alignment aims to align the output distribution (e.g., softmax probabilities) of the teacher and student [Hinton *et al.*, 2015; Zhao *et al.*, 2022; Zeng *et al.*, 2025]. For example, the multi-level logit distillation method [Jin *et al.*, 2023] employs multi-level prediction alignment to facilitate instance prediction learning in the student model. Curriculum temperature [Li *et al.*, 2023b] introduces temperature scheduling for dynamically adjusting softening intensity across training phases, which smooths gradient flow. The feature-level distribution alignment matches the representation, which is often done by maximum mean discrepancy, contrastive, and correlation-based loss [Gou *et al.*, 2021; Chen *et al.*, 2021]. Notable advancements in feature-level distillation encompass DiffKD [Huang

et al., 2023], training diffusion denoisers with teacher features to enforce attention map congruence in critical regions; WCoRD [Chen *et al.*, 2021], constructing global-local hybrid contrastive objectives with Wasserstein dual loss to align deep geometric structures. These alignment approaches have demonstrated effectiveness in knowledge transfer. Although there are some attempts by applying the decoupled distillation on the classification task [Zhao *et al.*, 2022; Li *et al.*, 2023a; Feng *et al.*, 2024]. There is no work on semi-supervised regression that more emphasizes how pseudo-labels are leveraged effectively. Another difference of our method is that we incorporate the adaptive learnable weighting scheme specifically for the non-target alignment to further prevent the student from overfitting noisy pseudo-supervision. Meanwhile, the continuous-valued knowledge is incorporated into the distribution alignment on the basis of label distribution learning and alignment, to keep the regression magnitude information.

3 Methodology

Notations. We assume the data set \mathcal{X} consists of n labeled samples $\mathcal{X}_l = \{(x_i, y_i)_{i=1}^n\}$ and m unlabeled samples $\mathcal{X}_u = \{(x_i)_{i=m}^{n+m}\}$, with instance $x \in \mathbb{R}$ for image, text, audio or tabular medical data. $\mathcal{Y} = \{y_i\}$ denotes the set of ground truth labels, where each label y_i is a continuous value in \mathbb{R} .

Problem Statement. Deep semi-supervised regression can be reformulated as given the training set \mathcal{X}_T and $\mathcal{X}_T = \mathcal{X}_l$, we aim to train a mapping function $f : \mathcal{X}_u \mapsto \mathcal{Y}$ which maps each input $x_i \in \mathcal{X}_u$ to a continuous scalar $y_i \in \mathbb{R}$. Semi-supervised learning explicitly incorporates unlabeled samples to complement limited labeled data during training. Therefore, in this case, the \mathcal{X}_T consists of \mathcal{X}_l and \mathcal{X}_u .

3.1 The Overview of DKD

As shown in Fig. 2, the proposed DKD predicts scores by establishing a decoupled representation distillation framework, where the ground truth is transformed into a label distribution, effectively converting the regression task into a discrete distribution estimation problem for both teacher and student models. We then apply DKD over the label distribution and DDA for the distribution alignment to enable the student model to learn fine-grained and more generalized knowledge.

This distillation process is particularly effective for the SSR task due to two key factors: (1) we reformulate the regression task as a distillation on both continuous-valued knowledge and distribution information in an end-to-end manner, which effectively mitigates the risk of the noise when integrating the pseudo labels, especially in the scenario that labeled samples are limited; and (2) we introduce a novel decoupled distribution alignment strategy for representation distillation over the classes, enabling the model to capture fine-grained features more effectively than conventional alignment methods. Finally, the model is jointly trained by combining the loss functions of the student and teacher, augmented with the proposed decoupled distribution alignment.

3.2 Distillation for Semi-supervised Regression

Label Distribution Learning Conventional SSR methods typically predict the score by directly mapping the input

sample x_i to the target value y . However, this approach is highly sensitive to noise and irrelevant features, often resulting in poor generalization and a high risk of overfitting, especially when few labels are available. Therefore, following [Gao *et al.*, 2017; Xu *et al.*, 2019], we define several classes $\mathcal{B} = \{\mathbf{b}_i\}_{i=1}^L$ based on the range of ground truth y , converting the regression task into a discrete distribution estimation problem. \mathcal{B} can be intuitively viewed as a set of evenly spaced score bins (anchors) that discretize the continuous regression label range into L classes, each covering an interval of width c , $\mathbf{b}_i = (i-1) \times c$, where each score is assigned to one corresponding class. Then, y can be obtained by calculating the expectation as follows:

$$y = \sum_{i=1}^L \tilde{p}_i \mathbf{b}_i \quad (1)$$

where \tilde{p}_i is the output probability of the model with the corresponding class \mathbf{b}_i . Therefore, the mapping function f in SSR is modified to learn a distribution $\mathcal{P} = \{p_i\}_{i=1}^L$ over predefined classes. By transforming the numerical regression into an interval prediction problem, it offers a smoother learning objective and richer label distribution than direct numerical regression [Xu *et al.*, 2019], leading to more effective use of limited labels and better noise robustness.

To obtain a probabilistic distribution, we apply the softmax function, and the predicted distribution is formulated as:

$$p_i = \frac{\exp(\tilde{p}_i)}{\sum_{i=1}^L \exp(\tilde{p}_j)} \quad (2)$$

where p_i is the predicted probability for the class \mathbf{b}_i after softmax. These outputs form a distribution, from which we compute the expectation to obtain the final score as follows:

$$\hat{y}_i = \sum_{i=1}^L p_i \mathbf{b}_i \quad (3)$$

Finally, we employ the MAE loss to minimize the distance between the prediction \hat{y}_i and the ground truth y_i :

$$\mathcal{L} = \frac{1}{|\mathcal{X}|} \sum_{x_i \in \mathcal{X}} |y_i - \hat{y}_i| \quad (4)$$

where y_i and the \hat{y}_i are the ground truth label and the predicted score of sample x_i , respectively. $|\mathcal{X}|$ is the number of samples in \mathcal{X} . In DKD, both the teacher and student models utilize the MAE loss function to incorporate supervised information, as detailed below.

Continuous-valued Knowledge Distillation Since using label distribution learning alone is insufficient for effective representation learning, we reformulate the knowledge distillation process to enable the student model to learn more generalized features for improved performance in SSR. To build the distillation framework for SSR, we first apply weak augmentation like random crop, flip, to the data before feeding it into the teacher model, while strong augmentation, like RandAugment [Cubuk *et al.*, 2020] is applied to the input of the student model. The detailed description of strong/weak augmentation on different domain data can be found in App. C.

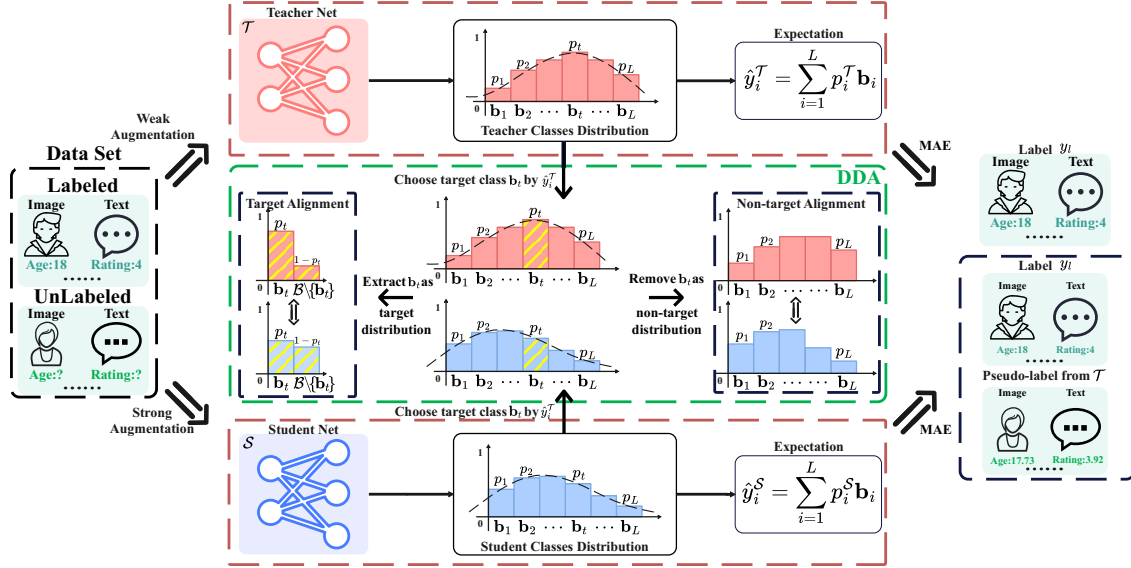


Figure 2: The Overview of DKD. (1) The input of DKD includes both labeled and unlabeled data. The teacher model is exclusively trained on the labeled data and is then used to generate pseudo labels for the unlabeled samples. The student model is trained on the entire dataset with a mixture of real labels and teacher-generated pseudo targets on unlabeled data. (2) Both the teacher and student are trained under a label-distribution formulation of regression, while continuous-valued distillation enforces consistency by minimizing the gap between their expected scores. (3) In the distribution distillation, DDA first identifies the target class to construct a binary probability distribution, then aligns the predicted distributions over classes between the teacher and student models separately for the target and non-target parts.

The predicted scores from the teacher model are used to guide the student by assigning corresponding pseudo-labels to the unlabeled nodes. As a result, the student model is trained on the entire dataset, including both labeled samples and unlabeled samples with pseudo-labels. The loss functions for the teacher and student models are thus defined separately as follows.

$$\mathcal{L}_T = \frac{1}{|\mathcal{X}_l|} \sum_{x_i \in \mathcal{X}_l} |y_i - \hat{y}_i^T| \quad (5)$$

$$\mathcal{L}_S = \frac{1}{|\mathcal{X}|} \sum_{x_i \in \mathcal{X}} |y_i - \hat{y}_i^S| \quad (6)$$

where \hat{y}_i^T and \hat{y}_i^S are the predicted scores of the teacher model and the student model, respectively. To enable the student model to learn more accurate information for SSR, we define the loss \mathcal{L}_{DKD} as follows, based on the joint training of the teacher and student models.

$$\mathcal{L}_{DKD} = \mathcal{L}_T + \mathcal{L}_S + \mathcal{L}_{Alignment} \quad (7)$$

The joint training mechanism enables the teacher model to generate high-quality pseudo labels from a small amount of labeled data, continuously improving the utilization of unlabeled data. The alignment loss $\mathcal{L}_{Alignment}$ minimizes the distance between the representations of the student and teacher models, typically implemented using Kullback–Leibler (KL) divergence or MSE. In DKD, we align the label distributions and further introduce a decoupled distribution alignment strategy, which will be described in the following sections.

3.3 Decoupling Distribution Alignment (DDA)

Conventional alignment methods often simply use KL divergence or MSE to minimize the distance between the teacher and student models. Although distillation helps the student exploit pseudo-labels in a more stable manner, simple alignment may be misled by noisy targets in pseudo-labeling data, yielding suboptimal performance [Mei *et al.*, 2023]. To mitigate this issue, we propose a DDA strategy that aligns the distributions over the classes at a more granular level, improving the student’s ability to fully exploit unlabeled samples and learn a better-calibrated regression model. Besides, aligning the distribution of discretized prediction classes is essential for effectively transferring knowledge from the teacher to the student. Furthermore, we empirically demonstrate that employing more advanced alignment strategies enables the student model to acquire richer and more effective knowledge, thereby enhancing the generalization ability of DKD.

Inspired by the success of decoupling target-level supervision from non-target relational insights in the classification task [Zhao *et al.*, 2022; Li *et al.*, 2024; Zheng and Cheng, 2025], we adopt a similar strategy to better exploit latent information from unlabeled samples in our SSR framework. Specifically, we first identify the target classes to formulate a binary classification task, treating the remaining classes as non-targets. The alignment is then performed separately on the target and non-target classes.

Target class identification. Since the entire dataset is fed into the teacher model, it is worth noting that the unlabeled samples do not provide supervision signals—only the labeled samples contribute to the MAE loss in the teacher

model. But in the advanced alignment, we choose to involve the unlabeled samples to provide more consistent information. Specifically, to determine the target class, we utilize the ground-truth labels for the labeled samples and the pseudo-labels for the unlabeled ones. In the presence of ground-truth labels, the target class \mathbf{b}_t is assigned to the corresponding label y_i ; otherwise, \mathbf{b}_t can be derived from the teacher's prediction \hat{y}_i^T . Furthermore, we denote the probability associated with the target class \mathbf{b}_t as p_t . The probability of the non-target set $\mathcal{B} \setminus \{\mathbf{b}_t\}$ is thus defined as $1 - p_t$.

Target and non-target class distribution alignment. Based on the identification of the target class, we can split the class into the target distribution to formulate the $\mathbf{p} = \{p_t, 1 - p_t\}$, with \mathbf{p}^T and \mathbf{p}^S to represent the teacher and student. The results of classes refer to the non-target distribution, *i.e.*, the remaining classes after excluding the target class, denoted as $\mathbf{q} = \{p_k\}_{k \neq t}^L$, with \mathbf{q}^T and \mathbf{q}^S to represent the teacher and student. The optimization of DDA can be reformulated as follows:

$$\mathcal{L}_{DDA} = \frac{1}{|\mathcal{X}|} \sum_{x_i \in \mathcal{X}} \text{KL}(\mathbf{p}_i^T, \mathbf{p}_i^S) + \beta \cdot \sum_{x_i \in \mathcal{X}} \omega_i \cdot \text{KL}(\mathbf{q}_i^T, \mathbf{q}_i^S) \quad (8)$$

where $\text{KL}(\mathbf{p}_i^T \parallel \mathbf{p}_i^S)$ aims to measure the similarity between the teacher distribution and student distribution on the target class, $\text{KL}(\mathbf{q}_i^T \parallel \mathbf{q}_i^S)$ is the similarity on the non-target class. β is the hyperparameter that controls the weights of no-target class alignment. For each sample, we introduce one learnable weight ω_i which is defined as $\max(1 - \sigma_i^T, 0)$, where σ_i^T is the standard deviation of teacher predictions. The key intuition is that incorporating this variance-aware weighting into the non-target class alignment allows the model to down-weight uncertain samples and focus the alignment on more reliable teacher guidance.

Compared with directly minimizing the KL divergence between teacher and student predictions on a mixture of labeled and pseudo-labeled samples, DDA performs decoupled alignment on target and non-target distributions, and introduces an adaptive learnable weighting scheme specifically for the non-target alignment. This prevents the student from overfitting noisy pseudo-supervision. As a result, DDA provides a more robust distribution alignment, enabling the student to better exploit unlabeled data under mixed supervision of ground-truth labels and pseudo targets.

3.4 Training and Inference

Training. During training, the DKD adopts the proposed distillation framework by jointly training the teacher and student model with corresponding loss functions \mathcal{L}_T and \mathcal{L}_S . The $\mathcal{L}_{Alignment}$ is implemented by the \mathcal{L}_{DDA} , defined as follows:

$$\mathcal{L}_{DKD} = \mathcal{L}_T + \mathcal{L}_S + \mathcal{L}_{DDA} \quad (9)$$

Inference. During inference, we solely use the student model to predict the score of a sample x_i in the test set \mathcal{X}_{Test} , as the student model is expected to learn rich and generalized knowledge from the teacher by leveraging the DDA. Give the unlabeled sample x_i in the \mathcal{X}_{Test} , the predicted score for the

unlabeled sample, denoted as \hat{y}_i :

$$\hat{y}_i = \sum_{i=1}^L p_i^S \mathbf{b}_i \quad (10)$$

where p_i^S is the prediction of the student model and \mathbf{b}_i is the value of the class.

4 Experiments

Datasets. We conduct experiments on four real-world regression benchmark datasets spanning computer vision, speech, natural language processing, and clinical data analysis: (1) BVCC [Cooper and Yamagishi, 2021] is an audio dataset that is utilized for predicting the perceptual quality of audio samples. (2) Yelp [Asghar, 2016] is a textual benchmark of customer reviews used to predict sentiment intensity. (3) UTK-Face [Zhang *et al.*, 2017b] is an image dataset used to estimate age from facial images. (4) MIMIC [Johnson *et al.*, 2023] is a medical tabular dataset that is used to predict the Sequential Organ Failure Assessment (SOFA) score. Table 1 summarizes their key statistics. More details about datasets are available in APP. A.

Model	BVCC	Yelp	UTKFace	MIMIC
# Train Set	4,974	250,000	18,964	3,623,503
# Test Set	1,066	25,000	4,741	55,859
Domain	Audio	Text	Image	Medical

Table 1: The statistical information of four datasets

Competing Methods. The competing methods can be categorized into three groups: direct regression, pseudo-label generation, and contrastive-learning-based approaches. (1) We directly predict the score by optimizing it using the MAE loss function, referred to as Direct Regression (DR). (2) The pseudo-label generation-based methods typically leverage the consistency regularization methods, including five technical approaches: perturbation-based self-ensembling frameworks, including π -model [Laine and Aila, 2017]; momentum-averaged teacher mechanisms with exponentially moving average, such as mean teacher [Tarvainen and Valpola, 2017]; co-training architectures like the dual-branch framework UCVME [Dai *et al.*, 2023a]; entropy-regularized constraint approaches typified by MixMatch [Berthelot *et al.*, 2019]; (3) The contrastive-learning-based methods leverage the ordinal relationships between unlabeled samples, including: the instance-level contrastive approach like CLSS [Dai *et al.*, 2023a]; GCLSS [Wang *et al.*, 2025] extends CLSS by leveraging a mixed similarity matrix from both labeled and unlabeled samples; RankUp [Huang *et al.*, 2024] improves SSR with an auxiliary ranking classifier. More details can be found in App. B.

Evaluation Metric. Following the previous work [Huang *et al.*, 2024; Dai *et al.*, 2023a], we adopt three widely used metrics to quantitatively assess the performance of DKD and other competing methods, including MAE, the correlation coefficient (R^2), and the Spearman Rank Correlation Coefficient (SRCC). MAE quantifies the average absolute deviation

Model	BVCC				Yelp				UTKFace				MIMIC		
	MAE ↓	R^2 ↑	SRCC ↑	MAE ↓	R^2 ↑	SRCC ↑	MAE ↓	R^2 ↑	SRCC ↑	MAE ↓	R^2 ↑	SRCC ↑	MAE ↓	R^2 ↑	SRCC ↑
DR	0.533	0.490	0.741	0.723	0.566	0.769	9.420	0.540	0.712	2.726	0.239	0.510			
π -Model (2017)	0.534	0.489	0.740	0.730	0.565	0.769	9.450	0.534	0.706	2.725	0.240	0.506			
Mean Teacher (2017)	0.532	0.492	0.742	0.730	0.565	0.769	8.850	0.586	0.745	2.724	0.240	0.507			
MixMatch (2019)	0.597	0.353	0.626	0.886	0.381	0.660	7.950	0.692	0.832	2.707	0.252	0.514			
CLSS (2023)	0.499	0.534	0.748	0.721	0.543	0.748	9.100	0.586	0.737	2.714	0.251	0.510			
UCVME (2023)	0.498	0.553	0.774	0.775	0.540	0.763	8.630	0.626	0.767	<u>2.656</u>	<u>0.285</u>	<u>0.539</u>			
RankUp (2024)	0.470	0.588	0.776	0.661	0.645	<u>0.829</u>	7.060	0.751	0.835	2.720	0.244	0.509			
GCLSS (2025)	<u>0.455</u>	<u>0.613</u>	<u>0.786</u>	<u>0.592</u>	<u>0.669</u>	0.821	<u>7.018</u>	<u>0.743</u>	<u>0.829</u>	2.934	0.135	0.374			
DKD (Ours)	0.422	0.669	0.818	0.549	0.694	0.839	6.852	0.761	0.838	2.629	0.291	0.541			

Table 2: The comparison results on four datasets. The best performance is boldfaced, with the second-best underlined.

between the model’s predictions and the true values. Lower MAE indicates better predictive accuracy. The SRCC quantifies the monotonic relationship between the predicted and ground-truth rankings, reflecting the proportion of variance in the target variable captured by the model.

Implementation Details. Our DKD model is implemented in Python 3.10 with PyTorch 2.1.2. All experiments are conducted on a GeForce RTX 4060 GPU with 8 GB of memory. The experimental configurations for DKD strictly adhere to those described in [Huang *et al.*, 2024]. In this paper, we set the default value of β to 10. We also adjust the β to explore its effectiveness, see Fig. 4. For all of the datasets. The number of classes L is set to 200 by default for the BVCC, Yelp, and UTKFace datasets and 100 for the MIMIC dataset. To ensure fair comparison across methods, we adopt the same augmentation schemes in RankUp [Huang *et al.*, 2024]. We apply weak augmentation to enrich the teacher’s knowledge, while strong augmentation is applied to the student to enhance generalization. More detailed parameter configurations and data augmentation mechanisms are provided in the App. C.

4.1 Main Comparison Results

Table 2 summarizes the performance of various methods across four datasets from four domains. All semi-supervised methods were trained on 250 labeled samples and evaluated on the test set. From the results, we observe that DKD significantly outperforms the tested SSR methods across all datasets. Specifically, DKD outperforms the second-best model, GCLSS, achieving significant overall improvements of 4.97% in MAE, 11.8% in R^2 , and 8.04% in SRCC across all datasets. Notably, GCLSS suffers a significant performance degradation on the MIMIC dataset. The possible reason is that GCLSS heavily relies on the feature similarity matrix, which is sensitive to the noise inherent in the MIMIC dataset derived from real-world ICU environments. Conversely, DKD achieves SOTA performance by fully leveraging unlabeled samples to learn more robust and generalizable knowledge representations through DDA.

The consistency regularization-based methods like the π -model, Mean Teacher, and MixMatch, which apply a consistency loss based on various data augmentations, consistently exhibit inferior performance across most datasets, merely matching the efficacy of DR on most datasets. The main reason is that their hybrid augmentation struggles to generate high-quality numeric pseudo-labels for the regression task,

particularly under extremely limited sample conditions. In contrast, DKD leverages decoupled distillation, thereby not only enhancing pseudo-label generation quality but also more effectively utilizing target and non-target distributions, which collectively improve its suitability for SSR tasks.

As for the co-trained method, UCVME, which maximizes variational mutual information, yields suboptimal results on the MIMIC dataset. However, it requires a more complex Bayesian neural network to perform uncertainty variational inference for real-valued pseudo-label refinement. In contrast, DKD distills knowledge from both continuous-valued knowledge and distribution information, consequently surpassing UCVME. Moreover, DKD also consistently outperforms CLSS by learning more generalized feature representations through superior distribution alignment.

4.2 Ablation Study

In this section, we perform an ablation study to evaluate the contribution of each component in DKD. We design three variants, including (1) Single-Label Distribution Learning (**S-LDL**), we remove the distillation framework, only keep the one branch, and train on the labeled samples. This is to evaluate the effectiveness of the proposed distillation framework. (2) **DKD-Logits**, which remove the DDA *i.e.*, only label alignment. (3) **DKD-KL**, which replaces the DDA with KL divergence. Both DKD-KL and DKD-Logits are used to evaluate the effectiveness of DDA. The results are shown in Table 3. From the results, the DKD can consistently outperform all the variants and yields the best performance on all the datasets, demonstrating its effectiveness. Both DKD-KL and DKD-Logits underperform the full DKD model but outperform S-LDL on the Yelp, UTKFace, and MIMIC datasets. This demonstrates that distillation effectively captures generalized patterns across text, image, and tabular medical data modalities. On the BCVV dataset, S-LDL achieves the second-best performance, though still behind DKD. This suggests that while S-LDL, leveraging only label distribution learning, can effectively learn patterns in audio data, the absence of distillation and DDA limits its ability, leading to suboptimal results.

4.3 Performance w.r.t. Labeled Sample Size

To explore the impact of labeled samples, we compare DKD with the competing methods, using varying numbers of labeled samples, with the results reported in Fig. 3. As the

Model	BVCC			Yelp			UTKFace			MIMIC		
	MAE ↓	R^2 ↑	SRCC ↑	MAE ↓	R^2 ↑	SRCC ↑	MAE ↓	R^2 ↑	SRCC ↑	MAE ↓	R^2 ↑	SRCC ↑
S-LDL	0.441	0.640	0.795	0.717	0.514	0.728	9.570	0.505	0.687	2.748	0.227	0.481
DKD-Logits	0.506	0.529	0.737	0.576	0.655	0.819	7.981	0.648	0.799	2.707	0.248	0.520
DKD-KL	0.500	0.547	0.747	0.610	0.617	0.8033	7.502	0.693	0.808	2.674	0.264	0.531
DKD (Ours)	0.422	0.669	0.818	0.549	0.694	0.839	6.852	0.761	0.838	2.629	0.291	0.541

Table 3: Ablation studies on the proposed model. The best performance is highlighted in bold, with the second-best underlined.

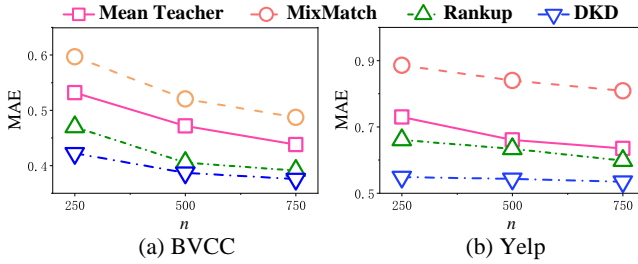


Figure 3: The MAE values w.r.t. of labeled sample size n .

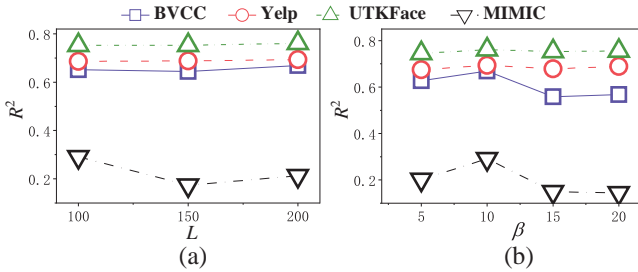


Figure 4: The effectiveness of hyperparameters L and β .

number of labeled instances n grows, DKD generally improves across the datasets, which is consistent with other tested semi-supervised methods. Across various labeling ratios, our DKD consistently achieves the best performance with the lowest MAE, demonstrating the robustness and efficacy of our proposed method.

4.4 Sensitive Analysis

We evaluate the sensitivity of DKD w.r.t. the hyperparameter class size L and β in \mathcal{L}_{DDA} . The results are shown in Fig. 4. More results can be found in App.D.

Performance w.r.t. Hyperparameter L : As shown in the Fig. 4(a), DKD performs stably under different classes on text, image, and audio datasets, and the performance slightly improves as L increases. The main reason lies in the capacity of larger classes to capture the intricate relationships within the label distribution more accurately. In contrast, on the MIMIC dataset, DKD achieved its highest performance with 100 classes, primarily because SOFA scores are more concentrated within a specific interval (typically around 4-10 in certain cohorts) compared to other datasets, and smaller classes are capable of capturing sufficient label information.

Performance w.r.t. Hyperparameter β in \mathcal{L}_{DDA} : As shown in the Fig. 4(b), DKD exhibited a consistent trend across all tested datasets, achieving optimal performance when beta was set to 10. The main reason is that a smaller β might cause the model to emphasize the 'difficulty' of train-

Model	MIMIC	Yelp	UTKFace	BVCC
UCVME (2023)	19	108	30	112
RankUp (2024)	10	28	43	46
GCLSS (2025)	8	23	12	36
DKD (ours)	15	34	150	66

Table 4: Runtimes (in seconds) on the four datasets.

ing samples, while a larger β forces it to learn more generalized non-target information from the student network. An effective balance is achieved when beta is set to 10.

4.5 Efficiency Analysis

Time Complexity In this section, we analyze the time complexity of DKD. Given that both models share the same backbone output as input, the computational cost of the backbone is excluded from this analysis. (1) The label distribution learning module comprises a fully connected layer and an expectation computation. Its time complexity is $\mathcal{O}(LM + 2L)$, where M denotes the dimension of the backbone output feature and L represents the number of classes. (2) The DKD consists of two components, including DDA and continuous-valued knowledge distillation. Their respective time complexities are $\mathcal{O}(L)$ and $\mathcal{O}(1)$ per sample. Consequently, the overall time complexity of DKD is $\mathcal{O}(N(2LM + 5L))$, where N is the number of samples.

Running Time Analysis. The runtimes of DKD and two recently proposed semi-supervised methods, including both training and inference time on NVIDIA GeForce GTX 4060, are reported in Table 4. DKD demonstrates higher efficiency on tabular medical data, text, and audio datasets. Although it requires more time on image datasets, this overhead is acceptable given the performance gains. Overall, DKD offers a favorable trade-off between efficiency and effectiveness.

5 Conclusion

In this paper, we propose DKD, the very first dual-stream knowledge distillation framework for fully exploiting the abundance of unlabeled samples and noise mitigation in pseudo-label supervision in SSR. DKD is designed to distill both continuous-valued knowledge and distribution information, which better preserves regression magnitudes and enhances the sample efficiency. Then, the DDA is proposed to further enhance the student's capacity to mitigate noise in pseudo-label supervision and learn a more well-calibrated regression predictor. Extensive experimental results across multiple datasets spanning four domains demonstrate that DKD outperforms state-of-the-art methods, indicating its superior generalization capability.

References

- [Asghar, 2016] Nabiha Asghar. Yelp dataset challenge: Review rating prediction. *arXiv preprint arXiv:1605.05362*, 2016.
- [Bao *et al.*, 2024] Jiaqi Bao, Mineichi Kudo, Keigo Kimura, and Lu Sun. Robust embedding regression for semi-supervised learning. *Pattern Recognition*, 145:109894, 2024.
- [Berthelot *et al.*, 2019] David Berthelot, Nicholas Carlini, Ian Goodfellow, Nicolas Papernot, Avital Oliver, and Colin A Raffel. Mixmatch: A holistic approach to semi-supervised learning. *Advances in neural information processing systems*, 32, 2019.
- [Chen *et al.*, 2021] Liqun Chen, Dong Wang, Zhe Gan, Jingjing Liu, Ricardo Henao, and Lawrence Carin. Wasserstein contrastive representation distillation. In *Proceedings of the IEEE/CVF conference on computer vision and pattern recognition*, pages 16296–16305, 2021.
- [Cooper and Yamagishi, 2021] Erica Cooper and Junichi Yamagishi. How do voices from past speech synthesis challenges compare today? In *11th ISCA Speech Synthesis Workshop (SSW 11)*, pages 183–188. ISCA, 2021.
- [Cubuk *et al.*, 2020] Ekin D Cubuk, Barret Zoph, Jonathon Shlens, and Quoc V Le. Randaugment: Practical automated data augmentation with a reduced search space. In *Proceedings of the IEEE/CVF conference on computer vision and pattern recognition workshops*, pages 702–703, 2020.
- [Dai *et al.*, 2023a] Weihang Dai, Yao Du, Hanru Bai, Kwang-Ting Cheng, and Xiaomeng Li. Semi-supervised contrastive learning for deep regression with ordinal rankings from spectral seriation. *Advances in Neural Information Processing Systems*, 36:57087–57098, 2023.
- [Dai *et al.*, 2023b] Weihang Dai, Xiaomeng Li, and Kwang-Ting Cheng. Semi-supervised deep regression with uncertainty consistency and variational model ensembling via bayesian neural networks. In *Proceedings of the AAAI Conference on Artificial Intelligence*, volume 37, pages 7304–7313, 2023.
- [Feng *et al.*, 2024] Shou Feng, Hongzhe Zhang, Bobo Xi, Chunhui Zhao, Yunsong Li, and Jocelyn Chanussot. Cross-domain few-shot learning based on decoupled knowledge distillation for hyperspectral image classification. *IEEE Transactions on Geoscience and Remote Sensing*, 2024.
- [Gao *et al.*, 2017] Bin-Bin Gao, Chao Xing, Chen-Wei Xie, Jianxin Wu, and Xin Geng. Deep label distribution learning with label ambiguity. *IEEE Transactions on Image Processing*, 26(6):2825–2838, 2017.
- [Gou *et al.*, 2021] Jianping Gou, Baosheng Yu, Stephen J Maybank, and Dacheng Tao. Knowledge distillation: A survey. *International journal of computer vision*, 129(6):1789–1819, 2021.
- [Gui *et al.*, 2024] Jie Gui, Tuo Chen, Jing Zhang, Qiong Cao, Zhenan Sun, Hao Luo, and Dacheng Tao. A survey on self-supervised learning: Algorithms, applications, and future trends. *IEEE Transactions on Pattern Analysis and Machine Intelligence*, 46(12):9052–9071, 2024.
- [Hinton *et al.*, 2015] Geoffrey Hinton, Oriol Vinyals, and Jeff Dean. Distilling the knowledge in a neural network. *arXiv preprint arXiv:1503.02531*, 2015.
- [Huang *et al.*, 2023] Tao Huang, Yuan Zhang, Mingkai Zheng, Shan You, Fei Wang, Chen Qian, and Chang Xu. Knowledge diffusion for distillation. *Advances in Neural Information Processing Systems*, 36:65299–65316, 2023.
- [Huang *et al.*, 2024] Pin-Yen Huang, Szu-Wei Fu, and Yu Tsao. Rankup: Boosting semi-supervised regression with an auxiliary ranking classifier. *Advances in Neural Information Processing Systems*, 37:107444–107468, 2024.
- [Jean *et al.*, 2018] Neal Jean, Sang Michael Xie, and Stefano Ermon. Semi-supervised deep kernel learning: Regression with unlabeled data by minimizing predictive variance. *Advances in Neural Information Processing Systems*, 31, 2018.
- [Jin *et al.*, 2023] Ying Jin, Jiaqi Wang, and Dahua Lin. Multi-level logit distillation. In *Proceedings of the IEEE/CVF Conference on Computer Vision and Pattern Recognition*, pages 24276–24285, 2023.
- [Jo *et al.*, 2024] Yongwon Jo, Hyungu Kahng, and Seoung Bum Kim. Deep semi-supervised regression via pseudo-label filtering and calibration. *Applied Soft Computing*, 161:111670, 2024.
- [Johnson *et al.*, 2023] Alistair EW Johnson, Lucas Bulgarelli, Lu Shen, Alvin Gayles, Ayad Shammout, Steven Horng, Tom J Pollard, Sicheng Hao, Benjamin Moody, Brian Gow, et al. Mimic-iv, a freely accessible electronic health record dataset. *Scientific data*, 10(1):1, 2023.
- [Laine and Aila, 2017] Samuli Laine and Timo Aila. Temporal ensembling for semi-supervised learning. In *International Conference on Learning Representations*, 2017.
- [Li *et al.*, 2023a] Yong Li, Yuanzhi Wang, and Zhen Cui. Decoupled multimodal distilling for emotion recognition. In *Proceedings of the IEEE/CVF conference on computer vision and pattern recognition*, pages 6631–6640, 2023.
- [Li *et al.*, 2023b] Zheng Li, Xiang Li, Lingfeng Yang, Borui Zhao, Renjie Song, Lei Luo, Jun Li, and Jian Yang. Curriculum temperature for knowledge distillation. In *Proceedings of the AAAI Conference on Artificial Intelligence*, volume 37, pages 1504–1512, 2023.
- [Li *et al.*, 2024] Mingcheng Li, Dingkang Yang, Xiao Zhao, Shuaibing Wang, Yan Wang, Kun Yang, Mingyang Sun, Dongliang Kou, Ziyun Qian, and Lihua Zhang. Correlation-decoupled knowledge distillation for multi-modal sentiment analysis with incomplete modalities. In *Proceedings of the IEEE/CVF Conference on Computer Vision and Pattern Recognition*, pages 12458–12468, 2024.
- [Mei *et al.*, 2023] Zhen Mei, Peng Ye, Baopu Li, Tao Chen, Jiayuan Fan, and Wanli Ouyang. Denkd: Decoupled non-target knowledge distillation for complementing

- transformer-based unsupervised domain adaptation. *IEEE Transactions on Circuits and Systems for Video Technology*, 34(5):3220–3231, 2023.
- [Mohammadi Foumani *et al.*, 2024] Navid Mohammadi Foumani, Lynn Miller, Chang Wei Tan, Geoffrey I Webb, Germain Forestier, and Mahsa Salehi. Deep learning for time series classification and extrinsic regression: A current survey. *ACM Computing Surveys*, 56(9):1–45, 2024.
- [Pan *et al.*, 2024] Zhiyu Pan, Jiahao Cui, Kewei Wang, Yizheng Wu, and Zhiguo Cao. Pseudo label fusion with uncertainty estimation for semi-supervised cropping box regression. *IEEE Transactions on Multimedia*, 26:8157–8171, 2024.
- [Qiao *et al.*, 2022] Hezhe Qiao, Lin Chen, and Fan Zhu. Ranking convolutional neural network for alzheimer’s disease mini-mental state examination prediction at multiple time-points. *Computer Methods and Programs in Biomedicine*, 213:106503, 2022.
- [Ren *et al.*, 2022] Jiawei Ren, Mingyuan Zhang, Cunjun Yu, and Ziwei Liu. Balanced mse for imbalanced visual regression. In *Proceedings of the IEEE/CVF conference on computer vision and pattern recognition*, pages 7926–7935, 2022.
- [Tarvainen and Valpola, 2017] Antti Tarvainen and Harri Valpola. Mean teachers are better role models: Weight-averaged consistency targets improve semi-supervised deep learning results. *Advances in neural information processing systems*, 30, 2017.
- [Van Engelen and Hoos, 2020] Jesper E Van Engelen and Holger H Hoos. A survey on semi-supervised learning. *Machine learning*, 109(2):373–440, 2020.
- [Wang *et al.*, 2022] Yidong Wang, Hao Chen, Yue Fan, Wang Sun, Ran Tao, Wenxin Hou, Renjie Wang, Linyi Yang, Zhi Zhou, Lan-Zhe Guo, et al. Usb: A unified semi-supervised learning benchmark for classification. *Advances in Neural Information Processing Systems*, 35:3938–3961, 2022.
- [Wang *et al.*, 2025] Ce Wang, Weihang Dai, Hanru Bai, and Xiaomeng Li. Contrastive learning for semi-supervised deep regression with generalized ordinal rankings from spectral seriation. *IEEE Transactions on Pattern Analysis and Machine Intelligence*, pages 1–14, 2025.
- [Xie *et al.*, 2020] Qizhe Xie, Zihang Dai, Eduard Hovy, Thang Luong, and Quoc Le. Unsupervised data augmentation for consistency training. *Advances in neural information processing systems*, 33:6256–6268, 2020.
- [Xu *et al.*, 2019] Ning Xu, Yun-Peng Liu, and Xin Geng. Label enhancement for label distribution learning. *IEEE Transactions on Knowledge and Data Engineering*, 33(4):1632–1643, 2019.
- [Yang *et al.*, 2022] Xiangli Yang, Zixing Song, Irwin King, and Zenglin Xu. A survey on deep semi-supervised learning. *IEEE transactions on knowledge and data engineering*, 35(9):8934–8954, 2022.
- [Yang *et al.*, 2024] Yang Yang, Nan Jiang, Yi Xu, and De-Chuan Zhan. Robust semi-supervised learning by wisely leveraging open-set data. *IEEE Transactions on Pattern Analysis and Machine Intelligence*, 46(12):8334–8347, 2024.
- [Yin *et al.*, 2022] Yingda Yin, Yingcheng Cai, He Wang, and Baoquan Chen. Fishermatch: Semi-supervised rotation regression via entropy-based filtering. In *Proceedings of the IEEE/CVF Conference on Computer Vision and Pattern Recognition*, pages 11164–11173, 2022.
- [Zeng *et al.*, 2025] Guolei Zeng, Hezhe Qiao, Guoguo Ai, Jinsong Guo, and Guansong Pang. Normality calibration in semi-supervised graph anomaly detection. *arXiv preprint arXiv:2510.02014*, 2025.
- [Zhang *et al.*, 2017a] Xucong Zhang, Yusuke Sugano, Mario Fritz, and Andreas Bulling. Mpiigaze: Real-world dataset and deep appearance-based gaze estimation. *IEEE transactions on pattern analysis and machine intelligence*, 41(1):162–175, 2017.
- [Zhang *et al.*, 2017b] Zhifei Zhang, Yang Song, and Hairong Qi. Age progression/regression by conditional adversarial autoencoder. In *Proceedings of the IEEE conference on computer vision and pattern recognition*, pages 5810–5818, 2017.
- [Zhang *et al.*, 2025] Tianlun Zhang, Yuxuan Luo, Xizhao Wang, and Sam Kwong. Semi-supervised segmentation on medical images with pseudo label calibration and neural process. *Neural Networks*, page 107510, 2025.
- [Zhao and Wen, 2025] Tao Zhao and Kehao Wen. A variable-type fuzzy system approach based on high-confidence pseudo-labels for semi-supervised regression. *IEEE Transactions on Emerging Topics in Computational Intelligence*, 2025.
- [Zhao *et al.*, 2022] Borui Zhao, Quan Cui, Renjie Song, Yiyu Qiu, and Jiajun Liang. Decoupled knowledge distillation. In *Proceedings of the IEEE/CVF Conference on computer vision and pattern recognition*, pages 11953–11962, 2022.
- [Zhao *et al.*, 2025] Zhiqian Zhao, Yinghou Jiao, Yeyin Xu, Enrico Zio, Zhaobo Chen, and Runchao Zhao. A few-shot fine-grained fault diagnosis framework based on pseudo-supervised task representation. *Applied Soft Computing*, page 114508, 2025.
- [Zheng and Cheng, 2025] Bowen Zheng and Ran Cheng. Rethinking decoupled knowledge distillation: A predictive distribution perspective. *IEEE Transactions on Neural Networks and Learning Systems*, pages 1–15, 2025.
- [Zheng *et al.*, 2025] Na Zheng, Xuemeng Song, Xue Dong, Aashish Nikhil Ghosh, Liqiang Nie, and Roger Zimmermann. Language-assisted debiasing and smoothing for foundation model-based semi-supervised learning. In *Proceedings of the Computer Vision and Pattern Recognition Conference*, pages 25708–25717, 2025.

A Datasets

A detailed introduction of all the datasets used in our work is given as follows.

BVCC [Cooper and Yamagishi, 2021] serves as an audio quality assessment benchmark, where the objective is to predict the perceptual quality of audio samples. Annotated on a 1-to-5 scale, the labels represent averaged scores from multiple listeners. This dataset comprises 4,974 training samples, 1,066 validation samples, and 1,066 test samples. Following the protocol defined in Rankup [Huang *et al.*, 2024], we exclusively utilize the training and validation splits for performance evaluation.

Yelp [Asghar, 2016] focuses on textual opinion mining, targeting the prediction of customer ratings based on reviews posted on the Yelp platform. The five-class rating labels represent distinct satisfaction levels. We employ the preprocessed Yelp data provided in the USB codebase [Huang *et al.*, 2024], consisting of 250,000 training samples, 25,000 validation samples, and 10,000 test samples. Consistent with RankUp’s methodology, only the training split is used for model training, while evaluation is performed on the validation set.

UTKFace [Zhang *et al.*, 2017b] addresses image-based age estimation, aiming to predict the age of individuals depicted in facial images. The age labels range from 1 to 116 years. RankUp partitions this dataset into 18,964 training samples and 4,741 test samples, with experiments conducted on its aligned and cropped version.

MIMIC [Johnson *et al.*, 2023] presents a multivariate time-series score prediction task, where the objective is to forecast SOFA scores (indicating illness severity from 0 to 24) based on patients’ clinical features over time. This dataset contains 3,623,503 training samples and 55,859 test samples.

Models	Wide ResNet-28-2	Whisper Base	Bert Small	Bert
Training Iterations	262,144	102,400	102,400	1024,000
Evaluation Iterations	1,024	1,024	1,024	1,024
Batch Size	32	8	8	8
Optimizer	SGD	AdamW	AdamW	AdamW
Momentum	0.9	-	-	-
Criterion	MAE	MAE	MAE	MAE
Weight Decay	1e-03	2e-05	5e-04	2e-5
Layer Decay	1.0	0.75	0.75	0.75
Learning Rate	1e-02	2e-06	1e-05	2e-06
EMA Weight	0.999	-	-	0.999
Pretrained	False	True	True	False
Sampler	Random	Random	Random	Random
Image Resize	40x40	-	-	-
Max Length Seconds	-	6.0	-	-
Sample Rate	-	16,000	-	-
Max Length	-	-	512	-

Table 5: The default hyperparameters for the base models.

B Competing Methods

A more detailed introduction of the six competing models and the evaluation metrics adopted in our work is given as follows.

B.1 Description of Baselines

π -Model [Laine and Aila, 2017] achieves self-ensembling by aggregating the outputs of a single network at different training stages. Consensus predictions for unknown labels are formed through diverse regularization and augmentation strategies. Perturbations are injected into both branches, and consistency between the two perturbed outputs is enforced, ensuring a more balanced and symmetric comparison.

Mean Teacher [Tarvainen and Valpola, 2017] aims to train a model via consistency between original samples and their perturbed counterparts, while using an exponential-moving-average (EMA) version of the model—termed the teacher—to supply more reliable guidance to the current student during training.

MixMatch [Berthelot *et al.*, 2019] consolidates the dominant approaches in semi-supervised learning by generating low-entropy label guesses for augmented unlabeled examples and subsequently blending labeled and unlabeled data via MixUp.

UCVME [Dai *et al.*, 2023b] improves training by producing high-quality uncertainty estimates for pseudo-labels via heteroscedastic regression. By explicitly modeling label uncertainty, the approach assigns greater importance to more reliable pseudo-labels. Furthermore, a novel variational model-ensembling scheme is introduced to reduce predictive noise and generate stronger pseudo-labels.

CLSS [Dai *et al.*, 2023a] extends contrastive regression to the semi-supervised domain. It exploits a spectral ordering algorithm to extract ordinal rankings from the feature-similarity matrix of unlabeled data and then leverages these rankings as supervisory signals. The additional ranking loss enhances robustness, marking the first exploration of contrastive learning for regression tasks.

RankUp [Huang *et al.*, 2024] reframes the original regression task as a ranking problem and trains it jointly with the regression objective. By introducing an auxiliary ranking classifier whose outputs can be handled by any off-the-shelf semi-supervised classification method, RankUp seamlessly integrates existing classification techniques into regression-oriented semi-supervised learning.

GCLSS [Wang *et al.*, 2025] extended CLSS to allow both labeled and unlabeled data to be used in the semi-supervised setting. Particularly, GCLSS uses labeled samples to regularize and rectify the recovered ordinal rankings of unlabeled data. The recovered rankings serve as pseudo-labels to supervise both the feature representations and the final predictions.

B.2 Evaluation Metric

We used Mean Absolute Error (MAE), R^2 , and Spearman’s Rank Correlation Coefficient (SRCC) as evaluation metrics for the tested model. The calculation process for each metric is as follows:

MAE: measures the average magnitude of the errors in a set

Models	π -Model	MeanTeacher	MixMatch	UCVME	CLSS	GCLSS	RankUp	DKD
Unlabeled Batch Ratio	1.0	1.0	1.0	1.0	0.25	0.25	7.0	7.0
Regression Unlabeled Loss Ratio	0.1	0.1	0.1	0.05	-	-	-	-
Regression Unlabeled Loss Warmup	0.4	0.4	0.4	-	-	-	-	-
Mixup Alpha	-	-	0.5	-	-	-	-	-
Dropout Rate	-	-	-	0.05	-	-	-	-
Ensemble Number	-	-	-	5	-	-	-	-
CLSS Lambda	-	-	-	-	2.0	2.0	-	-
Labeled Contrastive Loss	-	-	-	-	1.0	1.0	-	-
Unlabeled Contrastive Loss	-	-	-	-	0.05	0.05	-	-
Unlabeled Rank Loss Ratio	-	-	-	-	0.01	0.01	-	-
ARC Unlabeled Loss Ratio	-	-	-	-	-	-	1.0	-
ARC Loss Ratio	-	-	-	-	-	-	0.2	-
Confidence Threshold	-	-	-	-	-	-	0.95	-
Temperature	-	-	-	-	-	-	0.5	-
The Number of Selected Features	-	-	-	-	-	-	7	-
β	-	-	-	-	-	-	-	10

Table 6: Specific hyperparameters for each semi-supervised regression method.

Dataset	Augmentation
UTKFace	Weak: Random Crop, Random Horizontal Flip Strong: RandAugment [Cubuk <i>et al.</i> , 2020]
BVCC	Weak: Random Sub-sample Strong: Random Sub-sample, Mask, Trim, Padding
Yelp	Weak: None Strong: Back-Translation [Xie <i>et al.</i> , 2020]
MIMIC	Weak: Random Masking Strong: Operation Group

Table 7: Data augmentation strategies for different datasets.

of predictions, defined as follows:

$$\text{MAE} = \frac{1}{N} \sum_{i=1}^N |\hat{y}_i - y_i|,$$

where N denotes the number of samples, \hat{y}_i is the model’s prediction, and y_i is the corresponding ground-truth.

R^2 measures the proportion of variance in the ground-truth labels that is captured by the model. It is defined as

$$R^2 = 1 - \frac{\sum_{i=1}^N (\hat{y}_i - y_i)^2}{\sum_{i=1}^N (\bar{y} - y_i)^2},$$

where \bar{y} is the mean of the ground-truth labels. R^2 ranges from $(-\infty, 1]$; higher values indicate superior explanatory power. Let $r(\hat{y})$ and $r(y)$ denote the ranks of predictions and labels, respectively. Then

SRCC is a non-parametric measure of the statistical dependence between the rankings of two variables.

$$\text{SRCC} = \frac{\text{cov}(r(\hat{y}), r(y))}{\sigma_{r(\hat{y})} \sigma_{r(y)}},$$

with $\text{cov}(\cdot, \cdot)$ and σ denoting covariance and standard deviation, respectively. SRCC ranges from $[-1, 1]$, where the value closer to 1 implies a stronger rank-order.

C Parameters and Data Augmentation

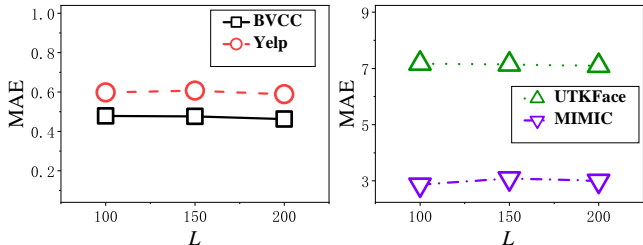
C.1 Parameter Configurations of Base Models

In this work, we employ a distinct base model for each database: Whisper-Base for audio data on BVCC, Bert-Small for text data on Yelp, Wide ResNet-28-2 for image data on UTKFace, and BERT for time-series prediction of SOFA values on MIMIC medical data. The common parameter Configurations of all the base models as listed in Table 5. Specific hyperparameter configurations for each SSR method are provided in Table 6.

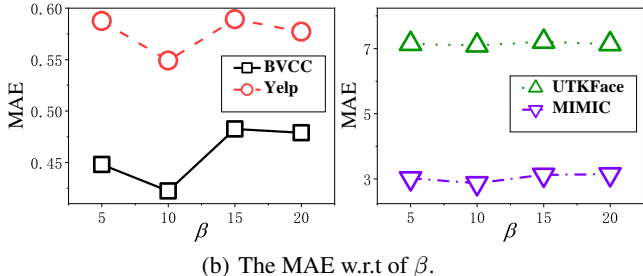
C.2 Weak and Strong Augmentation

For audio, image, and text data, we adopt the universal semi-supervised learning benchmark framework, USB [Wang *et al.*, 2022], to implement the weak and strong augmentations following the previous work [Huang *et al.*, 2024]. For the MIMIC dataset, given its time-series nature, weak augmentation involves applying random masking operations, while strong augmentation employs m rounds of random masking combined with Gaussian noise injection for multivariate time-series data. Specifically, each random masking operation obscures 5% of the observed data. Each Gaussian noise application introduces additive noise sampled from a normal distribution with zero mean and a variance of 0.02. To ensure fair comparison across methods, the same augmentation strategy is applied to both DKD and other comparative methods.

Detailed descriptions of data augmentation methods across different domains are presented in Table 7.



(a) The MAE w.r.t of bukets size L .



(b) The MAE w.r.t of β .

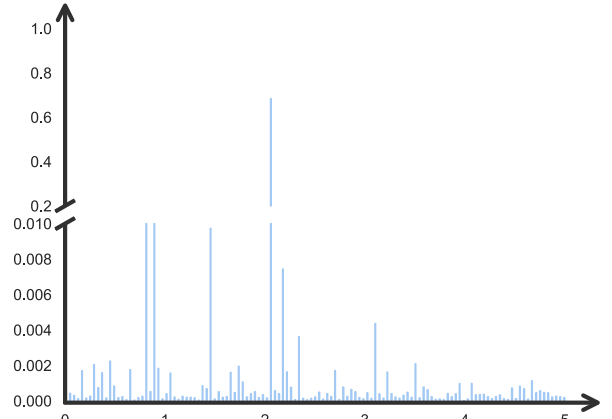
Figure 5: The effectiveness of the hyperparameters.

D Additional Experimental Results

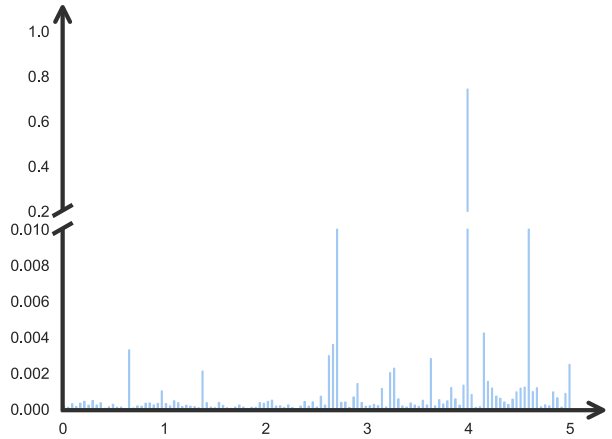
In this section, we further evaluate the effectiveness of the hyperparameters, specifically the class size of L and β , in \mathcal{L}_{DDA} using additional evaluation metrics. The results are shown in Fig.5. For the effectiveness of the class size L , compared to the R^2 , the MAE for DKD exhibits greater stability under variations of L , see Fig.5 (a). We found that the best performance is achieved with 200 classes for the BVCC, Yelp, and UTKFace datasets, while a lower MAE is obtained for the MIMIC dataset using 100 classes. Regarding the effectiveness of β in \mathcal{L}_{DDA} , see Fig.5 (b), the MAE demonstrates a trend comparable to that of R^2 across all datasets, with optimal performance universally observed at $\beta = 10$.

E Visualization Results

Fig. 6 presents a visualization of the prediction cases using the DKD model, illustrating the predicted discrete classes and their associated probability values on the Yelp dataset. As shown in Fig. 6 (a), for a regression value of 2, the Yelp dataset score prediction is made using a distributed set of $L=200$ classes that span the 0-to-5 rating range. Notably, in addition to the score of 2 (Fair/Dissatisfied) itself, the model primarily leverages the probabilities of the nearby related values of 1 (Poor/Very Dissatisfied) and 3 (Average/Neutral) for a combined prediction. A similar phenomenon can also be observed in the other example in Fig 6 (b). These results highlight DKD’s superior ability to exploit label information, which significantly enhances generalization and prevents overfitting.



(a) A prediction example of DKD with ground truth $y = 4$.



(b) A prediction example of DKD with $y = 2$.

Figure 6: The visualization results of DKD.